Progress in Relativistic Laser–Plasma Interaction with Kilotesla-Level Applied Magnetic Fields

K. Weichman,[1] A. P. L. Robinson,[2] M. Murakami,[3] J. J. Santos,[4] S. Fujioka,[3] T. Toncian,[5] J. P. Palastro,[1] and A. V. Arefiev[6,7]

[1]Laboratory for Laser Energetics, University of Rochester
[2]Central Laser Facility, STFC Rutherford Appleton Laboratory
[3]Institute of Laser Engineering, Osaka University, Japan
[4]University of Bordeaux, CNRS, CEA, CELIA, France
[5]Institute for Radiation Physics, Helmholtz-Zentrum Dresden-Rossendorf, Germany
[6]Department of Mechanical and Aerospace Engineering, University of California, San Diego
[7]Center for Energy Research, University of California, San Diego

Recent advances in vacuum magnetic-field–generation techniques[1–6] have renewed interest in the fundamentals of laser–plasma interaction in the presence of strong magnetic fields. In part, this interest has been motivated by the potential for applied magnetic fields to benefit applications of laser–plasma interaction at relativistic intensity ($I_0 \sim 10^{18}$ W/cm^2 for ~1-μm wavelength), including ion acceleration, inertial fusion energy, and the laboratory study of astrophysical phenomena. This summary builds on recent progress in understanding the basic physics of relativistic laser–plasma interaction with kilotesla-level applied magnetic fields: surface magnetic fields and the diamagnetic effect in laser–solid interaction, the effect of embedded magnetic fields on plasma expansion and ion acceleration, and magnetic-field–associated changes in the direct laser acceleration of electrons.

First, although plasma is conventionally considered diamagnetic and often acts to exclude magnetic fields, laser–plasma interactions have long been known to self-generate strong fields[7] and amplify applied magnetic fields.[8] The spatial localization of hot-electron production from an overdense target and the presence of a neutralizing cold return current offer additional opportunities for magnetic-field generation and amplification associated with kinetic electron dynamics, among which is surface magnetic-field generation arising from the inability of the hot-electron current to change the applied field in a conductive opaque target.[9] This surface magnetic field can influence later plasma dynamics including target expansion[9] and may reverse the sign of the magnetic field generated by laser-driven implosions when it is destabilized.[10] The latter case is of particular interest as a platform for extreme magnetic-field amplification. However, the process underlying the sign reversal phenomenon[10,11] has yet to be conclusively settled. This work introduces a computationally efficient model that is predictive of the sign of the magnetic field produced in implosions. This model demonstrates correlation between sign reversal in cylindrical implosions and instability of the surface magnetic field in a simplified planar configuration (Fig. 1).

Second, until recently, the effect of applied magnetic fields on laser-driven plasma expansion and ion acceleration has primarily been studied in the context of astrophysical jet dynamics[12] involving long time-scale (~nanosecond) evolution in sub-100-tesla magnetic fields, which necessitates magnetohydrodynamic modeling and eliminates the consideration of kinetic effects. The sheath-based ion-acceleration regime driven by short, relativistic intensity laser pules, on the other hand, is conducive to multidimensional kinetic modeling. Recent work in this regime has revealed the possibility of using an applied magnetic field to reverse the typical outward divergence associated with target normal sheath acceleration into focusing and improving the ion energy and number.[13,14] In this case, ion focusing, which is highly desirable and much studied under nonmagnetized conditions, is produced by eventual magnetization of the electron sheath as the plasma expands.[14] Observing ion focusing experimentally, however, will require the spatial scale of the applied magnetic field to be comparable to or greater than the focal length. This work introduces

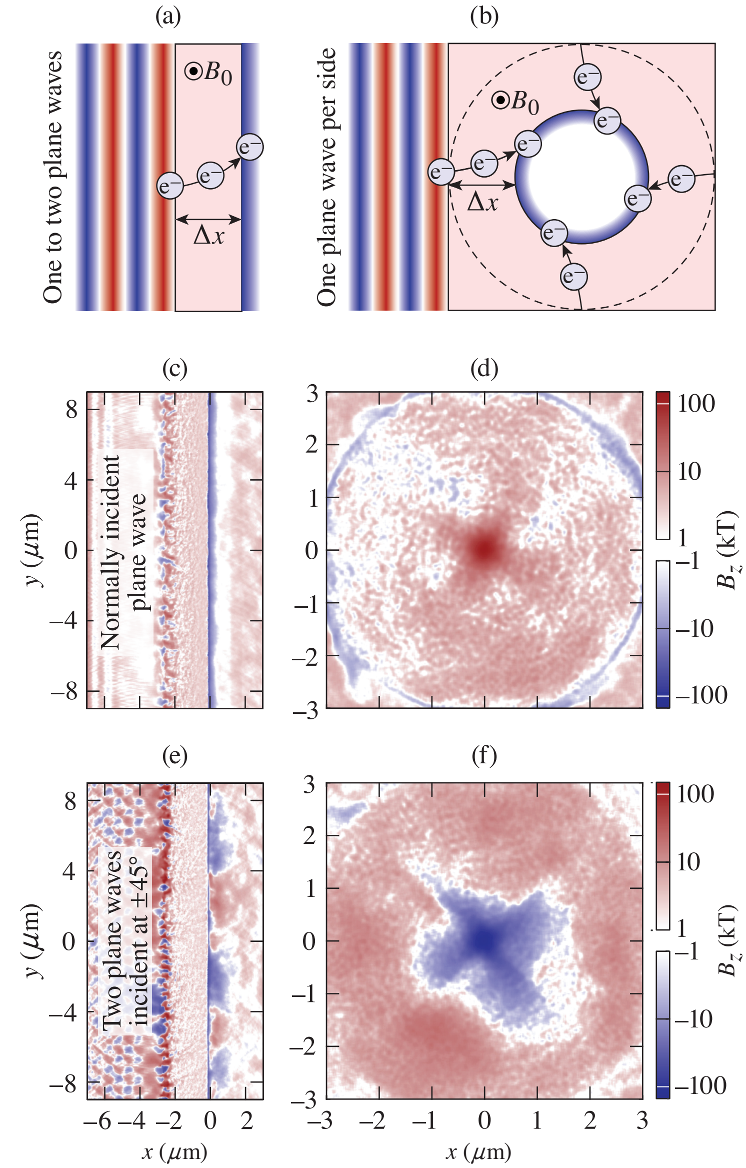

Figure 1
Planar model capturing surface magnetic-field stability and sign of the amplified field in implosions. [(a),(b)] Schematic of surface magnetic-field generation in (a) a planar target and (b) an implosion target with either square (solid line) or circular (dashed line) outer cross section. (c) Stable surface magnetic field in a planar target with normally incident plane wave pulse and (d) seed-aligned amplified magnetic field in a square implosion target. (e) Unstable surface magnetic field in a planar target with two obliquely incident pulses and (f) an amplified field in a circular implosion target.

a simple scaling model for sheath magnetization and subsequent ion focusing (Fig. 2). From this, realistic ion focal lengths are predicted that are likely compatible with the spatial extent of currently available applied magnetic fields.

Finally, while conventional electron acceleration mechanisms typically leave the majority of electrons cold either spectrally or spatially after the laser pulse has passed, direct laser acceleration (DLA) with an applied magnetic field is capable of volumetrically heating electrons to relativistic energy.[15–17] In the regime where the applied magnetic field affects the acceleration dynamics in a single accelerating laser half-cycle,[18] even modestly relativistic laser pulses can deliver significantly relativistic electron energy ($\gamma \sim 10$ or more). A configuration employing a secondary laser pulse prior to the main accelerating pulse (to provide the preheating necessary to enter this regime) was recently demonstrated to heat the majority of electrons in a large plasma volume to nonperturbatively relativistic energy.[18] The resulting optically diagnosable, relativistically thermal plasma is highly desirable for fundamental experimental studies in basic plasma physics, astrophysics and laboratory astrophysics, and laser-plasma physics. This work obtains an estimate for the average electron energy generated via magnetically assisted DLA (Fig. 3), which suggests plasma heating is most efficient for long, low (relativisitic)-intensity laser pulses.

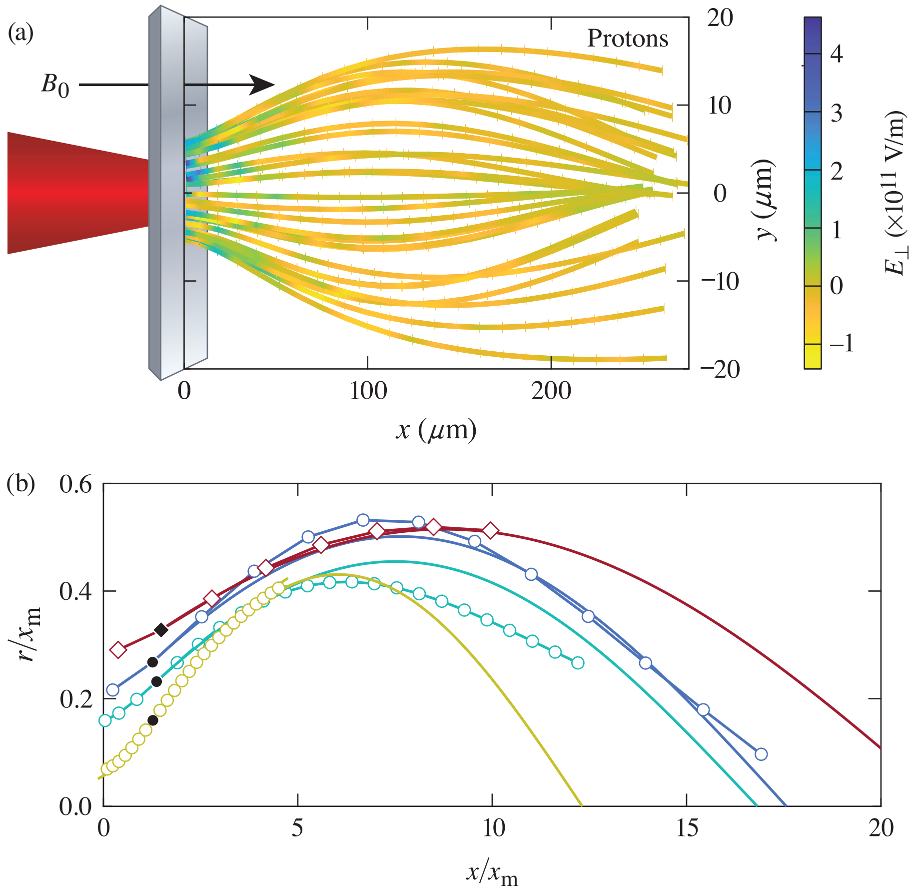

Figure 2
Model of ion focusing in magnetized electron sheath acceleration. (a) Schematic of ion acceleration with a target-normal applied magnetic field with proton trajectories. (b) Average high-energy proton trajectories from simulations keeping the laser waist divided by B_0 constant. $x_m \equiv (2\varepsilon_i T_e)^{1/2}/|e|B_0$.

Together, these results highlight the promise of applied magnetic fields in relativistic laser–plasma interactions. Current magnetic-field capabilities can already enable novel and highly desirable phenomena relevant to laser-plasma applications. The continual development of magnetic-field–generation techniques supports these efforts by opening new parameter regimes to exploration.

This material is based upon work supported by the Department of Energy National Nuclear Security Administration under Award Number DE-NA0003856, the University of Rochester, and the New York State Energy Research and Development Authority. A.V.A. was supported by NSF Grant No. 1903098. A.V.A. was supported by NSF Grant No. 1903098. The support of DOE does not constitute an endorsement by DOE of the views expressed in this paper. Particle-in-cell simulations were performed using *EPOCH*,[19] developed under UK EPSRC Grant Nos. EP/G054940, EP/G055165, and EP/G056803. This work used HPC resources of the National Energy Research Scientific Computing Center (NERSC), a U.S. Department of Energy Office of Science User Facility operated under Contract No. DE-AC02-05CH11231 using NERSC award FES-ERCAP-0021627, and the Extreme Science and Engineering Discovery Environment (XSEDE),[20] which is supported by National Science Foundation grant number ACI-1548562, under allocation TG-PHY210072 on the Texas Advanced Computing Center (TACC) at The University of Texas at Austin.

1. S. Fujioka *et al.*, Sci. Rep. **3**, 1170 (2013).
2. J. J. Santos *et al.*, New J. Phys. **17**, 083051 (2015).
3. L. Gao *et al.*, Phys. Plasmas **23**, 043106 (2016).
4. C. Goyon *et al.*, Phys. Rev. E **95**, 033208 (2017).
5. V. V. Ivanov *et al.*, Rev. Sci. Instrum. **89**, 033504 (2018).
6. G. Fiksel *et al.*, Rev. Sci. Instrum. **86**, 016105 (2015).
7. Z. M. Sheng and J. Meyer-ter Vehn, Phys. Rev. E **54**, 1833 (1996).

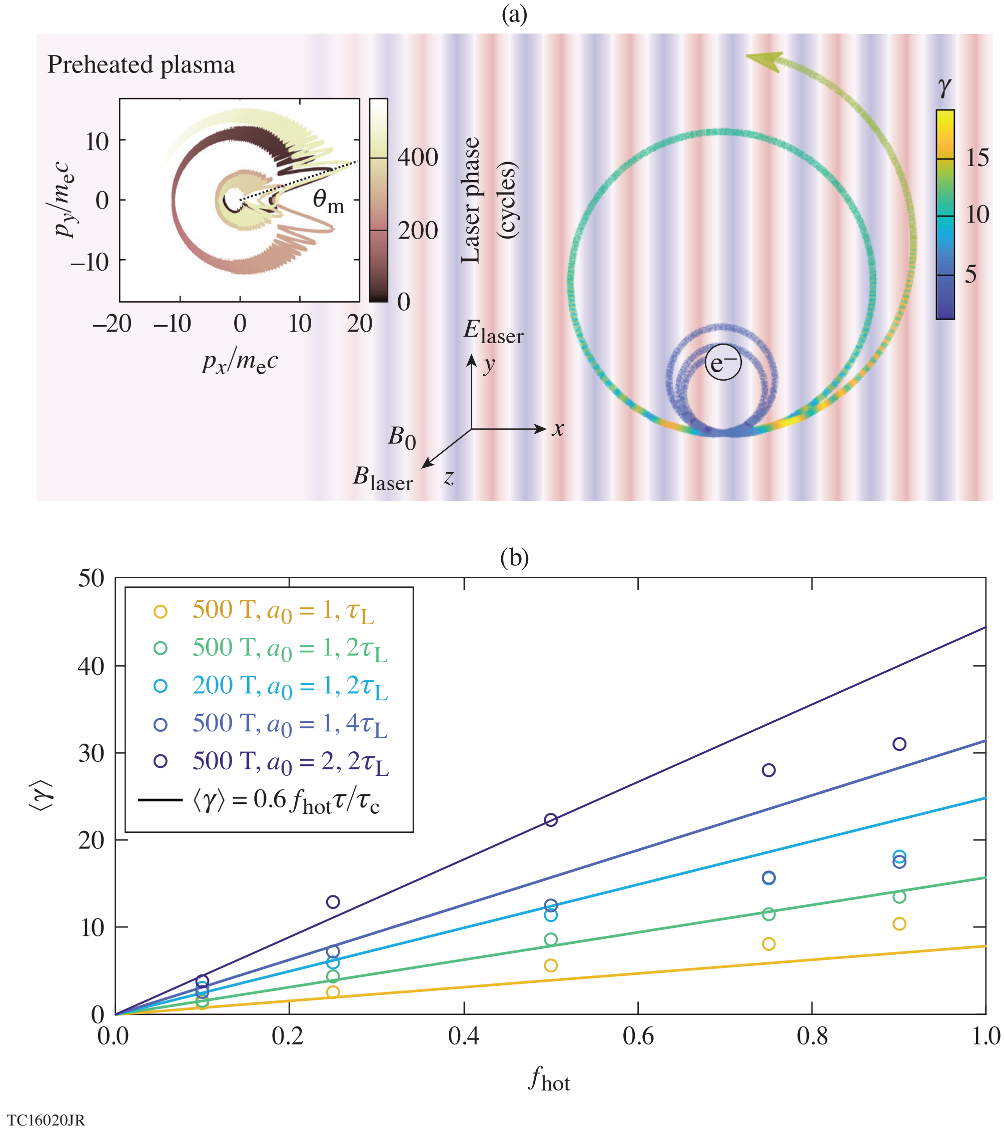

Figure 3
Half-cycle magnetically assisted direct laser acceleration in a preheated plasma. (a) Example of the many-kick electron acceleration process. (b) Average electron energy from particle-in-cell simulations varying the initial fraction of electrons above the the threshold for energy gain (f_{hot}). τ, τ_L, and τ_C are the pulse duration, the maximum Larmor period after a single kick, and the non-relativistic cyclotron period, respectively.

8. O. V. Gotchev *et al.*, Phys. Rev. Lett. **103**, 215004 (2009).
9. K. Weichman *et al.*, New J. Phys. **22**, 113009 (2020).
10. K. Weichman *et al.*, Appl. Phys. Lett. **117**, 244101 (2020).
11. Y.-J. Gu and M. Murakami, Sci. Rep. **11**, 23592 (2021).
12. B. Albertazzi *et al.*, Science **346**, 325 (2014).
13. A. Arefiev, T. Toncian, and G. Fiksel, New J. Phys. **18**, 105011 (2016).
14. K. Weichman *et al.*, Sci. Rep. **10**, 18966 (2020).
15. A. V. Arefiev, A. P. L. Robinson, and V. N. Khudik, J. Plasma Phys. **81**, 475810404 (2015).
16. A. P. L. Robinson and A. V. Arefiev, Phys. Plasmas **27**, 023110 (2020).

17. K. Weichman *et al.*, "Underdense Relativistically Thermal Plasma Produced by Magnetically Assisted Direct Laser Acceleration," Physics Archive: https://doi.org/10.48550/arXiv:2202.07015 (2022).
18. A. Arefiev, Z. Gong, and A. P. L. Robinson, Phys. Rev. E 101, 043201 (2020).
19. T. D. Arber *et al.*, Plasma Phys. Control. Fusion **57**, 113001 (2015).
20. J. Towns *et al.*, Comput. Sci. Eng. **16**, 62 (2014).